
Image classification and retrieval with random depthwise signed convolutional neural networks

Yunzhe Xue

Department of Computer Science
New Jersey Institute of Technology
Newark, NJ 07102
yx277@njit.edu

Usman Roshan

Department of Computer Science
New Jersey Institute of Technology
Newark, NJ 07102
usman@njit.edu

Abstract

We study image classification and retrieval performance in a feature space given by random depthwise convolutional neural networks. Intuitively our network can be interpreted as applying random hyperplanes to the space of all patches of input images followed by average pooling to obtain final features. We show that the ratio of image pixel distribution similarity across classes to within classes and the average margin of the linear support vector machine on test data are both higher in our network’s final layer compared to the input space. We then apply the linear support vector machine for image classification and k -nearest neighbor for image similarity detection on our network’s final layer. We show that for classification our network attains higher accuracies than previous random networks and is not far behind in accuracy to trained state of the art networks, especially in the top- k setting. For example the top-2 accuracy of our network is near 90% on both CIFAR10 and a 10-class mini ImageNet, and 85% on STL10. In the problem of image similarity we find that k -nearest neighbor gives a comparable precision on the Corel Princeton Image Similarity Benchmark than if we were to use the last hidden layer of trained networks. We highlight sensitivity of our network to background color as a potential pitfall. Overall our work pushes the boundary of what can be achieved with random weights.

1 Introduction

Convolutional neural networks (CNNs) are the state of the art in image recognition benchmarks today [1]. Optimization methods such as stochastic gradient descent [2] combined with data augmentation [3], regularization [4], dropout and cutout [5, 6] have made CNNs the de-facto approach for accurate image recognition [7]. Interestingly, several of these methods involve randomness.

For example the dropout method [5] ignores a random set of nodes during training. The cutout method [6] masks random square patches in the input training images. Stochastic gradient descent randomly uses a single training example at a time (or mini batches) to obtain the gradient as opposed to computing it from the entire dataset. This method has been shown to converge to the global optimum for convex functions as we increase the number of iterations [8]. All of these methods use randomness to avoid overfitting during training and thus give better model generalization.

We ask the question ”what is the performance of a fully random network where training is performed only in the last layer?”. Specifically we explore depthwise convolutional neural network with thousands of random filters in each layer except for the final flattened one. Random weights have been explored previously in several studies [9, 10, 11] including generating images with random nets [12]. They show the importance of a network architecture in achieving high accuracies and connect unsupervised pre-training and discriminative fine tuning to architecture. We too demonstrate the variation in accuracy across different architectures, but our work goes further than previous random convolution nets in several ways.

First, is the motivation and structure of our network. We arrive at our depthwise structure by applying random hyperplanes to all patches of all input images and average pooling the output of all patches. We provide

empirical measurements that show images across and within classes are better represented than the input feature space.

Second, we show that our network attains high accuracies comparable to state of the art trained networks on popular benchmarks. Previous work on random weights has been limited to MNIST [13] and CIFAR10 [14] benchmarks that contain smaller images whereas we examine STL10 [15] and ImageNet [16] that contain larger images. On MNIST we have the same accuracy as previous random nets (above 99%) but on CIFAR10 we perform much better than previously reported.

Third, we show that for image similarity our network final layer combined with a single layer trained network performs competitively when compared to the final hidden layer of a fully trained network. The last hidden layers of convolutional neural networks have shown to perform well for image retrieval in several previous studies [17, 18, 19]. Here, we use the Corel-Princeton Image Similarity benchmark [20] and demonstrate comparable precision with our network to trained ones across different values of k in k -nearest neighbor.

Finally we highlight some limitations of our network in data augmentation and its sensitivity to background colors. Overall we push the envelope of random networks and show that accuracies much better than expected can be achieved.

2 Methods

We start with the motivation for our network followed by a brief review of convolutional neural networks before describing our contribution.

2.1 Motivation and intuition behind depthwise random convolutions

We provide motivation and intuition with a simple toy example in Figure 1. There we see four images I_0, I_1, I_2 , and I_3 containing various objects. Clearly images I_0 and I_1 are very similar to each other. Image I_2 is also similar since it contains common objects as I_0 and I_1 but they are in different positions. Image I_3 shares only one common object to the other images and thus is the most dissimilar. We seek a representation that would capture these similarities.

Suppose we divide each image into four equal quadrants (or patches) and consider four random hyperplanes H_0, H_1, H_2 , and H_3 in the space of all patches as shown in Figure 1. We place patches containing the same object nearby in the figure since they are likely to be similar in pixel values. For example the car in par-

titions I_{02}, I_{12}, I_{23} , and I_{32} are clustered in the lower left in the middle figure near the origin.

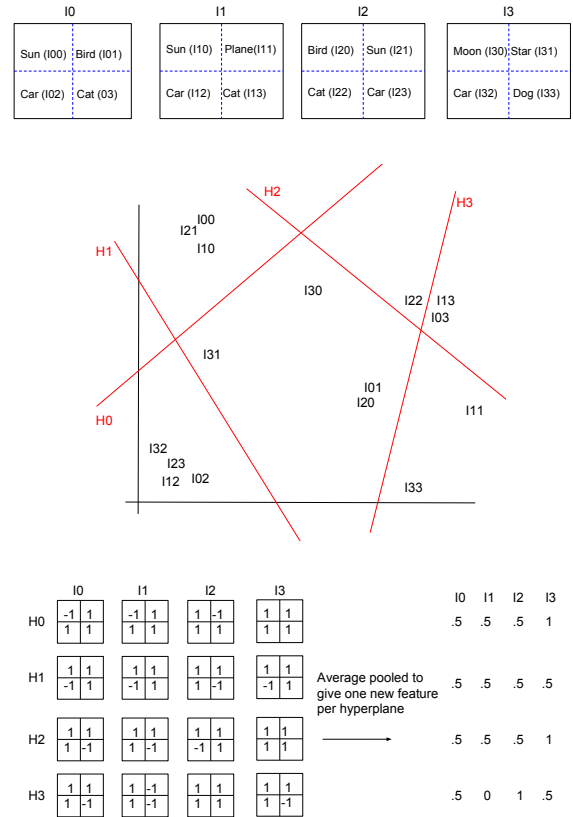


Figure 1: Shown in the top are four images each containing objects in different places of the image and divided into four partitions. In the middle we show four random hyperplanes (in red) on the input space of features from all patches of the images. The outputs of the four random hyperplanes correspond to a convolutional filter that considers just four partitions. We average pool to obtain a feature value.

We determine the sign of each patch according to each hyperplane and obtain a 2×2 matrix for each image. This is exactly the output of a convolution filter that considers just four partitions of an image. We then average pool the matrix to obtain a single feature value for the image given by the hyperplane. By repeating this for many hyperplanes we obtain more features per image. We see in our toy example that the final feature representation for images I_0, I_1 , and I_2 are more similar than image I_3 .

Instead of four patches we could simply run a convolutional kernel specifying a patch size (such as 5×5)

and obtain a second layer as we show in our example. Instead of average pooling that layer we could repeat the same process and apply another convolution. In a traditional network the new convolution would be applied across all images in the previous layer. However, our approach is depthwise and we apply the convolution to just the image in the previous layer in the same channel.

We don't have a theoretical guarantee that applying random hyperplanes to image patches repeatedly (as we do in our network) would yield a linearly separable space. However, one can draw intuition from our toy example in Figure 1. There we see that the four random hyperplanes partition the space and that patches in the same space will have exactly the same outputs for all four hyperplanes. Patches in adjacent partitions are likely to be less similar and will have exactly one of the four hyperplane outputs to be different. As we proceed to further patches the outputs of the hyperplanes will change even more.

We partition the space with random hyperplanes and find that as we add more hyperplanes the accuracy improves. We can say that adding hyperplanes further differentiates image similarity since we create more partitions. It is unclear at this time how to add new hyperplanes in a minimal way that produces the same differentiation in the space as many random ones.

2.2 Convolutional neural networks

Convolutional neural networks are typically composed of alternating convolution and pooling layers followed by a final flattened layer. A convolution layer is specified by a filter size and the number of filters in the layer. Briefly, the convolution layer performs a moving non-linearized dot product against pixels given by a fixed filter size $k \times k$ (usually 3×3 or 5×5). The dot product is usually non-linearized with the sigmoid or hinge (relu) function since both are differentiable and fit into the gradient descent framework. The output of applying a $k \times k$ convolution against a $p \times p$ image is an image of size $(p - k + 1) \times (p - k + 1)$.

The effect and advantage of convolution can be understood by considering all $k \times k$ patches of input training images and performing unsupervised learning on the patches [15]. This captures local similarity between images and allows for much better generalization than if we considered images as flattened input feature vectors. For example suppose we have two images containing a cat but in opposite corners. If we compared the patches of the two images we would find a cat in common. Previously Coates et. al. [15] performed k-means clustering [21] on such patches to obtain a new feature space for the input images on which they then

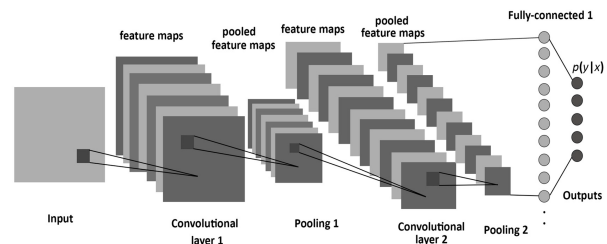


Figure 2: A typical convolutional neural network taken from [23].

apply a linear support vector machine [22]. Similar patches are likely to fall in the same cluster and this cluster membership determines the new feature space where images are compared by their local similarity.

A key thing to note is that the convolution performs the dot product through all layers of a given image. For example if an input image as m layers (for color RGB images $m = 3$) the dot product by the filter is applied to all layers and summed in the end. In the depthwise approach the i^{th} convolution filter is applied only to the i^{th} layer of the image.

In Figure 2 [23] we see a typical convolutional neural network with two convolution and two pooling layers. The pooling layers serve to reduce dimensionality which makes it easier to train the network. All the weights of the convolution filters and the final flattened layer are usually trained via stochastic gradient descent.

2.3 Random depthwise convolutional neural networks

Our work is inspired by successes of random weights in single layer neural networks [24, 25] and other unsupervised deep representation methods [15]. There, a linear classifier such as least squares or logistic regression is applied to the representation given by (non-linearized) outputs of a single layer network with random weights [24, 26]. We attempt to learn a feature space with random depthwise convolutions on which we then apply a linear support vector machine or stochastic gradient descent.

Our network is parameterized by the number of layers l , the size of each filter $k \times k$ and the number of filters m in each layer (this is the same in each layer). In Figure 3 we show an example of our network with two layers ($l = 2$) and five 3×3 convolution filters in each layer ($m = 5, k = 3$). We set the values in each filter randomly from the Normal distribution with mean 0 and variance 1.

We non-linearize the output of each convolution with

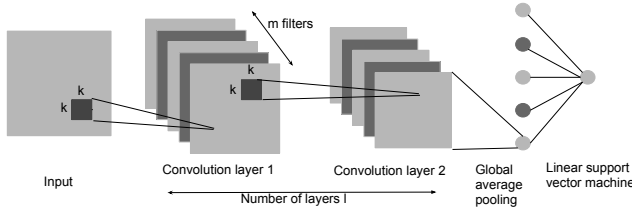


Figure 3: A random depthwise convolutional neural network with two layers, filter size of k , and $m = 5$ filters in each layer

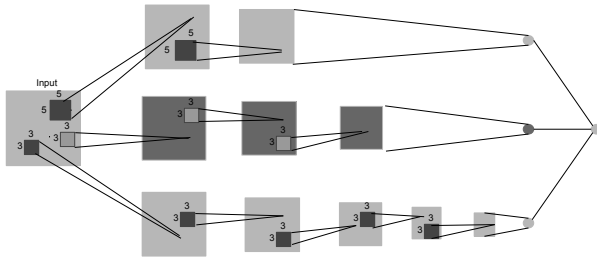


Figure 4: A hybrid random depthwise convolutional neural network with different number of layers and kernel size across the filters.

the sign function. Our convolution, however, is depthwise. This means the i^{th} convolution is applied on the i^{th} filter only of the previous layer. In the input layer, however, the convolution is applied in the conventional way to account for RGB images that have three layers.

After we are done with convolutions we globally average pool the final layer which gives us a flattened feature space. We then apply a linear support vector machine or stochastic gradient descent.

We also explore the use of hybrid models where the number of layers varies across each filter. In this extension the m^{th} filter has l_m layers and its own filter size k_m . In the example shown in Figure 4 we a network where the first filter has 3 layers ($l_0 = 3$), the second one has 5 layers ($l_1 = 5$), and the third one has 2 ($l_2 = 2$). The first two filters have sizes 3×3 and the third one is 5×5 .

2.4 Experimental performance study

In order to evaluate the empirical performance of our random network we compare it to three trained networks on several image benchmarks.

2.4.1 Deep networks compared in our study

We compare our method to modern networks in image recognition today. These are all convolutional neural networks designed to enable deeper architec-

tures and are trained with stochastic gradient descent. We implement these networks ourselves with Tensorflow and make our implementations freely available from the study website <https://github.com/xyzacademic/RandomDepthwiseCNN>.

- ResNet18 [27]: Residual convolutional networks contain connections from previous layers and not just the last one.
- DensenNet40 [28]: Convolutional networks contain dense layers in between convolutions.
- VGG16 [29]: Deep convolutional neural network with layers of convolution and pooling.

2.4.2 Datasets

We collect several image benchmarks on which we evaluate our method.

- MNIST [30]: Handwritten digit recognition from 10 classes in 32×32 images, training size of 60,000 and test size of 10,000
- CIFAR10 [14]: Object recognition from 10 classes in 32×32 color images, training size of 50,000, test size of 10,000
- CIFAR100 [14]: As CIFAR10 except from 100 classes
- STL10 [15]: Object recognition from 10 classes in 96×96 color images, training size of 5000, and test size of 8000
- Mini-ImageNet [16]: We randomly select 10 classes from the benchmark giving a total of 12,730 training and 500 test color images each of size 256×256 . We provide these set of images on the study’s website at <https://github.com/xyzacademic/RandomDepthwiseCNN>.
- Corel Princeton Image Similarity [20]: Eight query images and their similar images ranked by humans. We provide the image benchmark on our study’s website <https://github.com/xyzacademic/RandomDepthwiseCNN>.

2.4.3 Experimental platform and source code

We conduct all experiments on computing nodes equipped with Intel Xeon E5-2630-v4 CPUs and NVIDIA Tesla P100 16GB Pascal GPUs. We implement our method to produce the final flattened layer with Tensorflow and make it available on this study’s website <https://github.com/xyzacademic/RandomDepthwiseCNN>. We also provide there our implementations of other networks that we study in this paper including code to generate adversarial examples.

2.4.4 Program parameters and training

We use the liblinear program [31] version 2.20 for determining a linear support vector machine on the final layer obtained by our model. Our liblinear parameters are -s 2 -B 1 which turns on primal optimization and a threshold value of non zero. Our C (regularization) parameter values are 0.5 for CIFAR10, CIFAR100, and STL10, and 0.01 for MNIST and Mini-ImageNet. We optimize ResNet18, DenseNet40, and VGG16 networks with stochastic gradient descent. For CIFAR10 and CIFAR100 we use a batch size of 256 whereas for STL10 and Mini-ImageNet we use 32 and 16 respectively. On Mini-ImageNet we use 90 epochs and on the other benchmarks we use 300. We vary the learning rate across the number of epochs by starting with a large value of 0.1 and progressively reducing to 0.01 and 0.001 as the number of epochs increases.

3 Results

3.1 Hybrid models with different layers

We start by exploring the effect of combining models with different number of layers. In Table 4 we show the accuracy of our model with a fixed number of layers, fixed filter size, and 100,000 filters. In the last column we show the accuracy of a hybrid model. In STL10 and Mini-ImageNet this model is given by 25,000 filters of size $k = 3$ for each number of layers $l_0 = 7, l_1 = 11, l_2 = 15, l_3 = 21$. In the CIFAR10 hybrid model we also have 100,000 filters. There for each filter we randomly select the filter size between 3 and 5 and number of layers between between 3 and 9 for filter size 3 and between 2 and 4 for filter size 5.

We see that the hybrid model gives a better accuracy than a fixed number of layers in all three benchmarks. We also see a difference in accuracy across different number of layers with fixed filter size. A filter size of 5 and many layers significantly deteriorates performance on CIFAR10 and STL10, both of which have smaller images than Mini-ImageNet.

Table 1: Accuracy of our fixed vs hybrid models. Each model has a total of 100,000 filters. IN is short for ImageNet.

Dataset	filter size $k = 3, l = \text{layers}$				hybrid
	$l=7$	$l=11$	$l=15$	$l=21$	
STL10	66	67.9	69	69	71.3
Mini IN	75	74.4	75	72.8	78
	$l=2$	$l=5$	$l=7$	$l=9$	
CIFAR10	71.8	73.8	73.9	73.6	78.4

3.2 Effect of number of random filters on test accuracy

Having established that the hybrid model is better than fixed layers we proceed to determine the effect of number of filters on the test accuracy. Each filter gives rise to a new feature in the final flattened layer. We expect an improvement in test accuracy as we increase the number of filters and indeed we see this is the case in Figure 5(a). There we see that increasing the number of filters improves the accuracy on the STL10 and CIFAR10 benchmarks. We also see that the train accuracy reaches 100% much faster and stays there while test accuracy continues to improve.

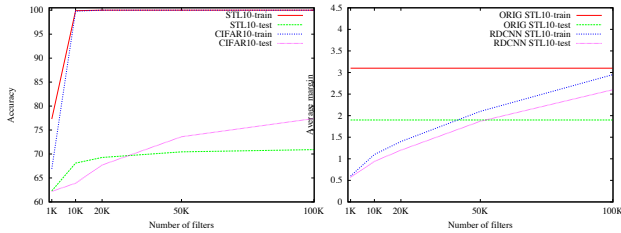
3.3 Comparison of margin before and after our network

We conjecture that the new feature space given by our network makes the images better linearly separable thus giving good results with the linear support vector machine. Following the definition of the geometric margin [32] we measure the average margin of the support vector machine defined as $\frac{1}{n} \sum_i y_i \frac{(w^T x_i + w_0)}{\|w\|}$. Note that the geometric margin is the minimum value of this term below across all i . The term multiplying the label $y_i \in \{-1, 1\}$ is the signed distance of the feature vector x_i to the hyperplane given by vector w and scalar threshold w_0 [33], and n is the number of training examples. For misclassified points the product term is negative and for correctly classified points it is positive. Thus the larger the term the better separated the points from two classes are.

We select the first two classes in the STL10 benchmark and study the margins between them on our final data representation. In Figure 5(b) we see that the separation between the two classes (given by the average margin) in both train and test are similar and increase as we increase the number of filters. We also see that the margin on the train data is higher in the original space but the test data margin is lower than the one given by our network.

3.4 Image pixel distribution similarity across and within classes

We select 10 random images from STL-10 (6 from class 0 and 4 from class 1) and show the distribution of the image pixel values before and after our network. In Figure 6(a) we see the distribution of image pixel values in the original data and in (b) we show the distribution in our final layer before the SVM. We see that the random filters smoothen the image distributions and appear to show a better separation of image distributions between the two classes.



(a) Effect on accuracy (b) Effect on average margin

Figure 5: Effect of number of filters (final features) on the test accuracy and the average margin

In order to obtain a quantitative measure we report the average Jensen Shannon (avgJS) divergence [34] between image pixel distributions across classes and within classes. To obtain this we simply average the divergence across all pairs of image distributions across two classes (and within classes). We then measure the ratio of

$$\frac{avgJS(class0, class1)}{avgJS(class0, class0) + avgJS(class1, class1)}$$

For images in the original feature representation we find a ratio of $\frac{0.25}{0.3+0.18} = 0.52$ and in our RDCNN final layer the ratio increases to $\frac{0.02}{0.018+0.016} = 0.59$. This ratio varies across classes and the above values are for class 0 and 1 that we randomly chose. If we measure this ratio between classes 0 and 6 we see a larger difference in the ratio across the two feature representations. In the original representation this value is $\frac{0.24}{0.3+0.13} = 0.56$ and in our RDCNN final layer it increases to $\frac{0.025}{0.018+0.015} = 0.76$. Thus we see that our new feature representation gives a better *signal to noise* ratio.

3.5 Image classification benchmark results

Before going into the accuracies we first list below our best model on each dataset.

- MNIST: One layer, filter size 7×7
- CIFAR10: Hybrid model of 100,000 filters. In each filter we randomly select the filter size between 3 and 5 and number of layers between between 3 and 9 for filter size 3 and between 2 and 4 for filter size 5.
- CIFAR100: Same as above

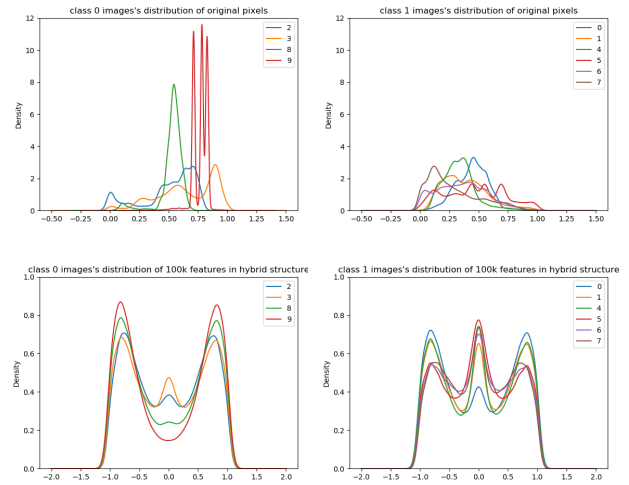


Figure 6: Pixel distribution of images from two classes in the original and new representations

- STL10: Hybrid model of 100,000 filters. We have 25,000 filters of size $k = 3$ for each number of layers $l_0 = 7, l_1 = 11, l_2 = 15, l_3 = 21$.
- Mini ImageNet: Same as above

In Figure 7 we show the test accuracies of the top-1, top-2, and top-3 outputs from all networks on four benchmarks. The top-k outputs are obtained by considering images with the top k highest outputs in the final layer. In our case we use the SVM discriminant to rank the outputs.

In STL10 our random network performs comparably to trained networks without data augmentation. In fact it performs better than when DenseNet is trained without data augmentation. On the other benchmarks our network is trailing in accuracy but that difference becomes smaller as we consider top-2 and top-3 outputs of the classifier.

In both CIFAR10 and Mini ImageNet we see that the random network has the steepest increase in accuracy from top-1 to top-2. In fact in top-2 our network is about 90% accurate on CIFAR10 and Mini ImageNet and 85% on STL10. In CIFAR100 that has a 100 classes our network catches up to trained networks at a much slower pace.

In previous work on random networks Saxe et. al. [9] obtained 53.2% on CIFAR10 and Jarrett et. al. [10] 99.46% on MNIST. Our network reaches 71% on CIFAR10 and 99.4% on MNIST. Thus we perform better

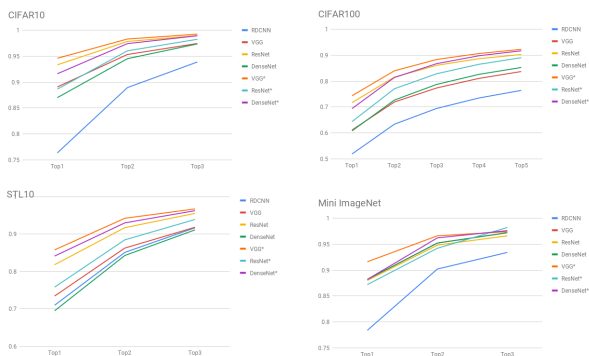


Figure 7: Top-k accuracy of different networks on benchmarks. Methods with asterisk denote data augmentation was enabled.

than previous random nets on CIFAR10 and comparably on MNIST.

Data augmentation For our method we first separately generated augmented images with flips and random rotations from STL10 (10 augments per input image). We then combined these into the original training set and used them as input to our network. Our final test accuracy, however, was no better than training on just the original data. To understand this compare the cosine similarity of each augmented image to its original and plot the cosine similarity value distribution across all images. We perform the cosine similarity in the feature space given by the final layer of our network. In Figure 8 we see that the flips and rotations produce images that are highly similar to the original in our feature representation. However, if we perform the cutout augmentation [6] the images are relatively more different. Perhaps this augmentation or something even stronger may boost the accuracy of our network.

3.6 Image similarity benchmark results

We train the VGG16 and ResNet18 networks on all images in the Corel Princeton Image Similarity dataset [20] except for the eight queries. In this benchmark the most similar images are ranked and given a score by human observers. We use the last hidden layer for representing all images. Our choice for this comes from previous studies that have shown the final hidden layer (that is usually a dense layer) works best for image retrieval with deep convolutional neural networks [19, 18, 17].

In the case of our random network we use the final

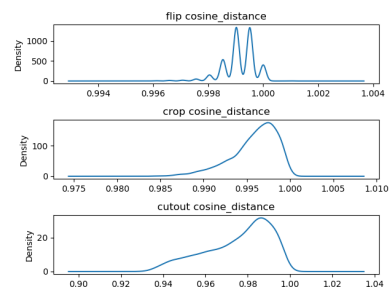


Figure 8: Cosine similarity distribution across all STL10 images. Each cosine value is between an image and its augmentation in our network’s final layer feature space.

layer of the hybrid model for STL10 to represent all images. We also study a version of our network where we perform some training. We feed the our final layer into a single layer multilayer perceptron with sigmoid activation and 1000 features in the hidden layer (as implemented in Python scikit-learn [35]). Here we exclude the eight queries from the training procedure.

We then obtain the top-k nearest neighbors for each of the eight queries in the four different feature spaces: two trained, one our random network followed by single layer network, and just random. For each value of k we determine the intersection ratio (also known as the precision) as the number of common images in the true top k images for the given query divided by k . In Figure 9 we see the intersection ratios for VGG16, Resnet18, our random network, and our network followed by a trained single layer neural network.

On the average across the eight queries our trained random network has the highest precision values as we cross values of k above 10. If we sum the score of all images in the intersection there too we see our trained network in the lead (bottom Figure 9). Our random one (without training) is behind VGG but better than ResNet.

While our method performs well for image similarity on this benchmark we see that the trained networks produce a better classification of the eight queries. We consider the correct classification of the query to be the category it belongs to in the database images. Both VGG and ResNet classify 7 out of 8 correctly whereas our random network does 6 out of 8 correctly. On the training VGG and ResNet achieve 98% accuracy whereas our trained random network gets to 76% with the multilayer perceptron.

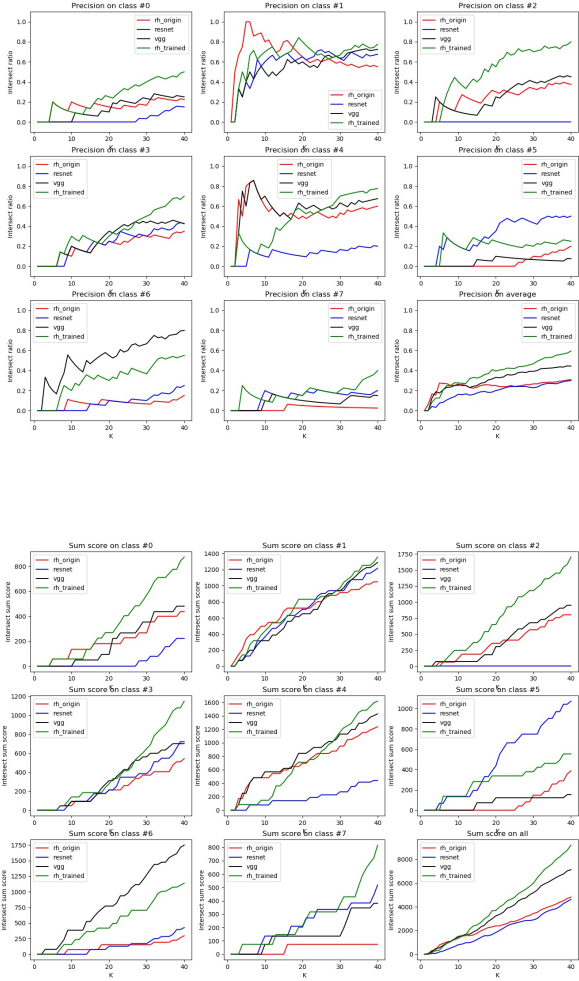


Figure 9: Shown here in the top is the intersection ratio (also known as precision) of top-k images returns in the feature space of each trained model. In the bottom are the sum of scores of images in the intersection.

4 Discussion

The importance of network architecture has been emphasized in previous work [36, 9, 10]. In support of previous results we also show variation in accuracy as the models vary and for the first time show superior performance given by hybrid models.

We found that our network is somewhat more sensitive to color than trained networks. From STL10 we pick a bird image and show the top similar images to it as given by VGG16 and our network. Here we measure

cosine similarity in final layer of VGG and our network. In the top Figure 10 we see that VGG reports almost all birds as the most similar image to the original bird. In our layer shown in the bottom of Figure 10 we see that images similar to the bird are also similar in color and mostly not birds.

Thus our random network is sensitive to color which possibly accounts for its trailing accuracy in classification tasks. In the image similarity benchmark it performs better with some training though. There it's likely the combination of its sensitivity to color (since similar images may have similar background colors) and training that produces better precision than a trained VGG network for the image similarity task.



Figure 10: Shown here are cosine similarity values of the top 16 images similar to the bird in the upper left. In the top are images from a trained VGG and in the bottom are images from our random network.

To determine the sensitivity of our method to training set size we reversed our Mini-ImageNet training and test: we use the much smaller test set of 500 images as training and 12,370 for test. In this experiment we found our method to give 58% accuracy while a trained ResNet18 gives 48% and 63.7% without and with data augmentation respectively.

5 Conclusion

We study random depthwise convolutional neural networks with thousands of convolutional filters per layer. We show that with the final layer of our network we can achieve competitive accuracies in image classification and retrieval while also highlighting some pitfalls.

References

- [1] Alex Krizhevsky, Ilya Sutskever, and Geoffrey E Hinton. Imagenet classification with deep convolutional neural networks. In F. Pereira, C. J. C. Burges, L. Bottou, and K. Q. Weinberger, editors, *Advances in Neural Information Processing Systems 25*, pages 1097–1105. Curran Associates, Inc., 2012.
- [2] Léon Bottou. Large-scale machine learning with stochastic gradient descent. In *Proceedings of COMPSTAT’2010*, pages 177–186. Springer, 2010.
- [3] Justin Salamon and Juan Pablo Bello. Deep convolutional neural networks and data augmentation for environmental sound classification. *IEEE Signal Processing Letters*, 24(3):279–283, 2017.
- [4] Quoc V Le. Building high-level features using large scale unsupervised learning. In *Acoustics, Speech and Signal Processing (ICASSP), 2013 IEEE International Conference on*, pages 8595–8598. IEEE, 2013.
- [5] Nitish Srivastava, Geoffrey Hinton, Alex Krizhevsky, Ilya Sutskever, and Ruslan Salakhutdinov. Dropout: A simple way to prevent neural networks from overfitting. *The Journal of Machine Learning Research*, 15(1):1929–1958, 2014.
- [6] Terrance DeVries and Graham W Taylor. Improved regularization of convolutional neural networks with cutout. *arXiv preprint arXiv:1708.04552*, 2017.
- [7] Alex Krizhevsky, Ilya Sutskever, and Geoffrey E Hinton. Imagenet classification with deep convolutional neural networks. In *Advances in neural information processing systems*, pages 1097–1105, 2012.
- [8] Noboru Murata. A statistical study of on-line learning. *Online Learning and Neural Networks*. Cambridge University Press, Cambridge, UK, pages 63–92, 1998.
- [9] Andrew M Saxe, Pang Wei Koh, Zhenghao Chen, Maneesh Bhand, Bipin Suresh, and Andrew Y Ng. On random weights and unsupervised feature learning. In *ICML*, pages 1089–1096, 2011.
- [10] Kevin Jarrett, Koray Kavukcuoglu, Yann LeCun, et al. What is the best multi-stage architecture for object recognition? In *Computer Vision, 2009 IEEE 12th International Conference on*, pages 2146–2153. IEEE, 2009.
- [11] Nicolas Pinto, David Doukhan, James J DiCarlo, and David D Cox. A high-throughput screening approach to discovering good forms of biologically inspired visual representation. *PLoS computational biology*, 5(11):e1000579, 2009.
- [12] Kun He, Yan Wang, and John Hopcroft. A powerful generative model using random weights for the deep image representation. In *Advances in Neural Information Processing Systems*, pages 631–639, 2016.
- [13] Yann LeCun, Corinna Cortes, and Christopher JC Burges. The mnist database of handwritten digits, 1998.
- [14] Alex Krizhevsky. Learning multiple layers of features from tiny images. 2009.
- [15] Adam Coates, Andrew Ng, and Honglak Lee. An analysis of single-layer networks in unsupervised feature learning. In *Proceedings of the fourteenth international conference on artificial intelligence and statistics*, pages 215–223, 2011.
- [16] Olga Russakovsky, Jia Deng, Hao Su, Jonathan Krause, Sanjeev Satheesh, Sean Ma, Zhiheng Huang, Andrej Karpathy, Aditya Khosla, Michael Bernstein, Alexander C. Berg, and Li Fei-Fei. ImageNet Large Scale Visual Recognition Challenge. *International Journal of Computer Vision (IJCV)*, 115(3):211–252, 2015.
- [17] Ji Wan, Dayong Wang, Steven Chu Hong Hoi, Pengcheng Wu, Jianke Zhu, Yongdong Zhang, and Jintao Li. Deep learning for content-based image retrieval: A comprehensive study. In *Proceedings of the 22nd ACM international conference on Multimedia*, pages 157–166. ACM, 2014.
- [18] Ali Sharif Razavian, Hossein Azizpour, Josephine Sullivan, and Stefan Carlsson. Cnn features off-the-shelf: an astounding baseline for recognition. In *Proceedings of the IEEE conference on computer vision and pattern recognition workshops*, pages 806–813, 2014.
- [19] Huafeng Wang, Yehe Cai, Yanxiang Zhang, Haixia Pan, Weifeng Lv, and Hao Han. Deep learning for image retrieval: What works and

- what doesn't. In *Data Mining Workshop (ICDMW), 2015 IEEE International Conference on*, pages 1576–1583. IEEE, 2015.
- [20] Corel-princeton image similarity benchmark. <http://www.cs.princeton.edu/cass/benchmark/>.
- [21] Adam Coates and Andrew Y Ng. Learning feature representations with k-means. In *Neural networks: Tricks of the trade*, pages 561–580. Springer, 2012.
- [22] Corinna Cortes and Vladimir Vapnik. Support-vector networks. *Machine learning*, 20(3):273–297, 1995.
- [23] Saleh Albelwi and Ausif Mahmood. A framework for designing the architectures of deep convolutional neural networks. *Entropy*, 19(6), 2017.
- [24] Yi Wang, Yi Li, Momiao Xiong, Yin Yao Shugart, and Li Jin. Random bits regression: a strong general predictor for big data. *Big Data Analytics*, 1(1):12, 2016.
- [25] Guang-Bin Huang, Qin-Yu Zhu, and Chee-Kheong Siew. Extreme learning machine: theory and applications. *Neurocomputing*, 70(1):489–501, 2006.
- [26] Yi Wang, Yi Li, Weilin Pu, Kathryn Wen, Yin Yao Shugart, Momiao Xiong, and Li Jin. Random bits forest: a strong classifier/regressor for big data. *Scientific Reports*, 6, 2016.
- [27] Kaiming He, Xiangyu Zhang, Shaoqing Ren, and Jian Sun. Deep residual learning for image recognition. In *Proceedings of the IEEE conference on computer vision and pattern recognition*, pages 770–778, 2016.
- [28] Gao Huang, Zhuang Liu, Kilian Q Weinberger, and Laurens van der Maaten. Densely connected convolutional networks. In *Proceedings of the IEEE conference on computer vision and pattern recognition*, volume 1, page 3, 2017.
- [29] Karen Simonyan and Andrew Zisserman. Very deep convolutional networks for large-scale image recognition. *arXiv preprint arXiv:1409.1556*, 2014.
- [30] Yann LeCun, Léon Bottou, Yoshua Bengio, and Patrick Haffner. Gradient-based learning applied to document recognition. *Proceedings of the IEEE*, 86(11):2278–2324, 1998.
- [31] Rong-En Fan, Kai-Wei Chang, Cho-Jui Hsieh, Xiang-Rui Wang, and Chih-Jen Lin. Liblinear: A library for large linear classification. *The Journal of Machine Learning Research*, 9:1871–1874, 2008.
- [32] Bernhard Schölkopf and Alexander J. Smola. *Learning with Kernels: Support Vector Machines, Regularization, Optimization, and Beyond*. MIT Press, Cambridge, MA, USA, 2001.
- [33] Ethem Alpaydin. *Machine Learning*. MIT Press, 2004.
- [34] Bent Fuglede and Flemming Topsøe. Jensen-shannon divergence and hilbert space embedding. In *Information Theory, 2004. ISIT 2004. Proceedings. International Symposium on*, page 31. IEEE, 2004.
- [35] F. Pedregosa, G. Varoquaux, A. Gramfort, V. Michel, B. Thirion, O. Grisel, M. Blondel, P. Prettenhofer, R. Weiss, V. Dubourg, J. Vanderplas, A. Passos, D. Cournapeau, M. Brucher, M. Perrot, and E. Duchesnay. Scikit-learn: Machine learning in Python. *Journal of Machine Learning Research*, 12:2825–2830, 2011.
- [36] Zhizhen Chi, Hongyang Li, Jingjing Wang, and Huchuan Lu. On the importance of network architecture in training very deep neural networks. In *Signal Processing, Communications and Computing (ICSPCC), 2016 IEEE International Conference on*, pages 1–5. IEEE, 2016.